

Seismic Reliability Analysis of Offshore Fixed Platforms Using Incremental Dynamic Analysis

Mohammadizadeh, M.R.^{1*}, Vahidi, K.² and Ronagh, H.R.³

¹ Assistant Professor, Department of Civil Engineering, Faculty of Engineering, University of Hormozgan, Bandar Abbas, Iran.

² M.Sc. Student, Department of Civil Engineering, Faculty of Engineering, University of Hormozgan, Bandar Abbas, Iran.

³ Professor, Centre for Infrastructure Engineering, Western Sydney University, Australia.

Received: 28 Apr. 2018;

Revised: 07 Aug. 2018;

Accepted: 19 Aug. 2018

ABSTRACT: It is generally accepted that performance-based design has to be reliability-based. Seismic performance evaluation is based on nonlinear dynamics and reliability theory taking into account uncertainties during analysis. Considering the economic importance of jacket type offshore platforms, the present research aims to assess the seismic performance of offshore steel platforms. In this study, three platforms located in the Persian Gulf were modeled using three dimensional structural modeling tools. Each platform was modeled and analyzed using both rigid and pinned connections. Reliability analysis was performed in accordance with Federal Emergency Management Agency (FEMA) guidelines using the results of incremental dynamic analysis for the three platforms. The results showed that platforms possessing rigid connections provide the desired confidence level of FEMA for the performance level of collapse prevention while only one platform with pinned connections was able to provide the desired confidence level.

Keywords: Incremental Dynamic Analysis, Offshore Platforms, Performance Levels, Seismic Behavior.

INTRODUCTION

In recent decades, massive investment has been made in marine oil and gas field development. During this time the offshore platform technology has developed considerably and made remarkable progress. Most common types of offshore platforms in the shallow and medium depth regions of Iranian waters are the steel jacket type platforms whose components are as follows (Management and Planning Organization of Iran 2006):

a) The jacket which is a space frame structure

consisting of welded tubular members that is designed as a template used to install piles and provide a bracing system; b) The piles that permanently connect the jacket to seabed and tolerate vertical and lateral loads; c) The superstructure or deck that possesses the structure needed to provide the desired performance of the platform.

In performance based earthquake engineering, seismic capacity and demand must be determined both in order to evaluate structural performance. Performance evaluation of nonlinear systems is a complex process and appropriate analytical

* Corresponding author E-mail: mrzmohammadizadeh@yahoo.com

methods have to be used for modeling the behavior of the structure against earthquakes. Considering recent advances in computer analysis, it is possible to use non-linear dynamic analysis for this purpose. Incremental non-linear dynamic analysis (IDA) is a desirable indicator for the assessment of structures where seismic loads are scaled and gradually increased. The concepts behind this approach was first stated by Bertero (1977) and later developed by Vamvatsikos and Cornell (2002). Jacket platforms have been studied in some researches. For example, Pourgharibshahi and Hadavand Khani (2011) used IDA analysis to evaluate a platform located in the Persian Gulf conducting reliability analysis based on IM-based research performed by Ibarra and Krawinker (2005). Golafshani et al. (2009) compared the FEMA 356 (2000) and API (2000) approaches for assessment of jacket offshore platform structures. Komachi et al. (2009) presented the performance based assessment of jacket platforms for seismic vulnerability. Asgarian et al. (2008) investigated IDA results considering soil-pile interaction for a well-head platform in the Persian Gulf. Zolfaghari et al. (2015) compared the results of Static Pushover (SPO) analysis and Comprehensive Interaction IDA (CI-IDA) analysis for a six-leg platform. Asgarian and Ajamy (2010) used the IDA analysis to predict nonlinear behavior of three newly designed jacket type offshore platforms subjected to strong ground motions. Ventura et al. (2014) presented a novel methodology to incorporate uncertainties associated with seismic loads, characterization of structural model parameters and description of soil properties in the probabilistic assessment of seismic-related damage of existing jacket type offshore platforms.

Other investigations related to jacket type offshore platforms and relatively similar to IDA procedure include Probabilistic Incremental Wave Analysis (PIWA) which is used to assess the performance of jacket offshore platforms under extreme waves, e.g. Golafshani et al. (2011) and Hezarjaribi et al. (2013). There are also researches on Endurance Wave Analysis (EWA) for nonlinear dynamic analysis and assessment of offshore

structures, e.g. Zeinoddini et al. (2012) and Dastan Diznab et al. (2014). Investigations on seismic performance based evaluation of structures can be referred to Waseem and Spacone (2017), Khorami, et al. (2017), Bayat et al. (2015), Qiao et al. (2017), Mirtaheri et al. (2017), Davani et al. (2016), Yön, (2016), Maniyar et al. (2009), Bayat et al. (2017), Asgarian (2016), Sistani et al. (2013), Lee and Moon (2014), Mahmoudi et al. (2013), Abdollahzadeh and Malekzadeh (2013), Abdollahzadeh et al. (2015).

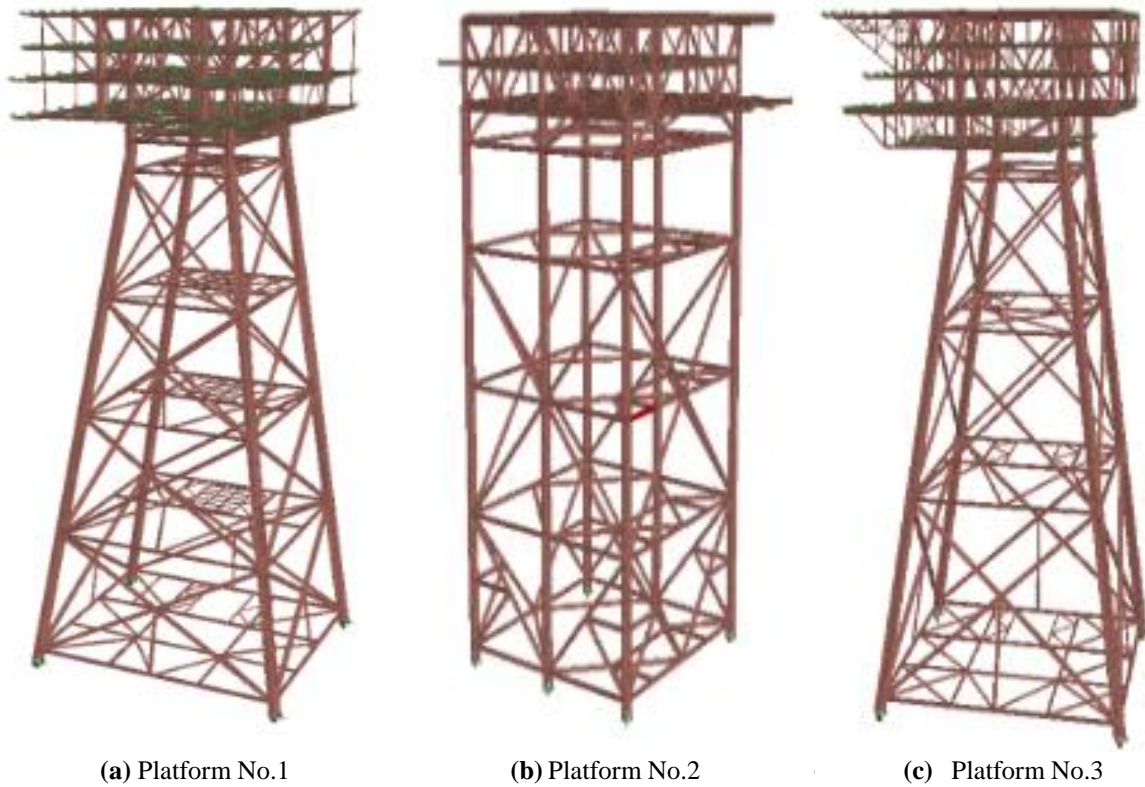
The present study contributes to the literature on the topic in that it covers some of the gaps in the abovementioned studies, i.e. seismic reliability assessment of platforms in two states, rigid connections and pin connections by applying earthquake forces due to ground motions in three directions simultaneously (in two orthogonally horizontal directions and in vertical direction) based upon FEMA procedures using IDA results.

INTRODUCTION OF STRUCTURES

Structural models for platforms are real three-dimensional models whose characteristics include jacket weight, deck weight and weight of attachments, the number of elements and nodes, total height and water depth at the platform installation site (Table 1). The platforms described in Table 1, were modeled and analyzed using SeismoStruct V6.5 software which is a free-share software for seismic structural analysis. In all models, the impact of waves on structures, which is negligible in earthquakes, was ignored and the connection of structure to the seabed was considered as being fixed. In the dynamic analysis, the weight of deck attachments was considered as nodal lumped masses. In addition, link elements were used to model the pinned connections. The three-dimensional model of platforms is shown in Figures 1(a)-(c). The jacket for platform number 1 is a 4-leg type including 5 horizontal braced levels located at heights of -69.60, -50, -31, -13 and +5.75. The deck comprises of 5 floors located at heights of +11.10, + 13.90, + 18.90, + 22.90 and +27.41. Figures 2(a)-(e) shows the plan of different

floors of the deck. The jacket for platform number 2 is a 6-leg type consisting of 5 horizontal braced levels located at heights of -68.50, -48, -28.5, -8.5 and +6.5. The deck is composed of 3 floors located at heights of +11.70 + 17.50 and +23.50. Different floor plans of the deck in platform number 2 have been shown in Figures 3(a)-(c). The jacket in

platform number 3 is a 4-leg type being composed of 4 horizontal braced levels located at heights of -61.60, -35, -13 and +5.75. The deck contains 5 floors located at heights of +10.10, + 14.25, +18.30, +21.85 and +25.51. Figures 4 (a)-(e) shows the plan of different floors in platform number 3.

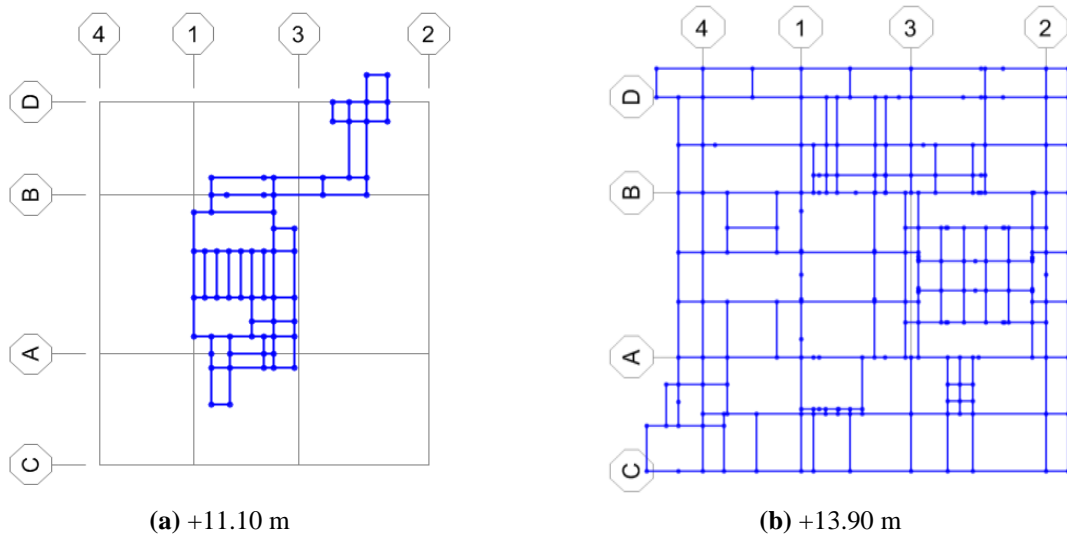


(a) Platform No.1

(b) Platform No.2

(c) Platform No.3

Fig. 1. Three-dimensional model of platforms



(a) +11.10 m

(b) +13.90 m

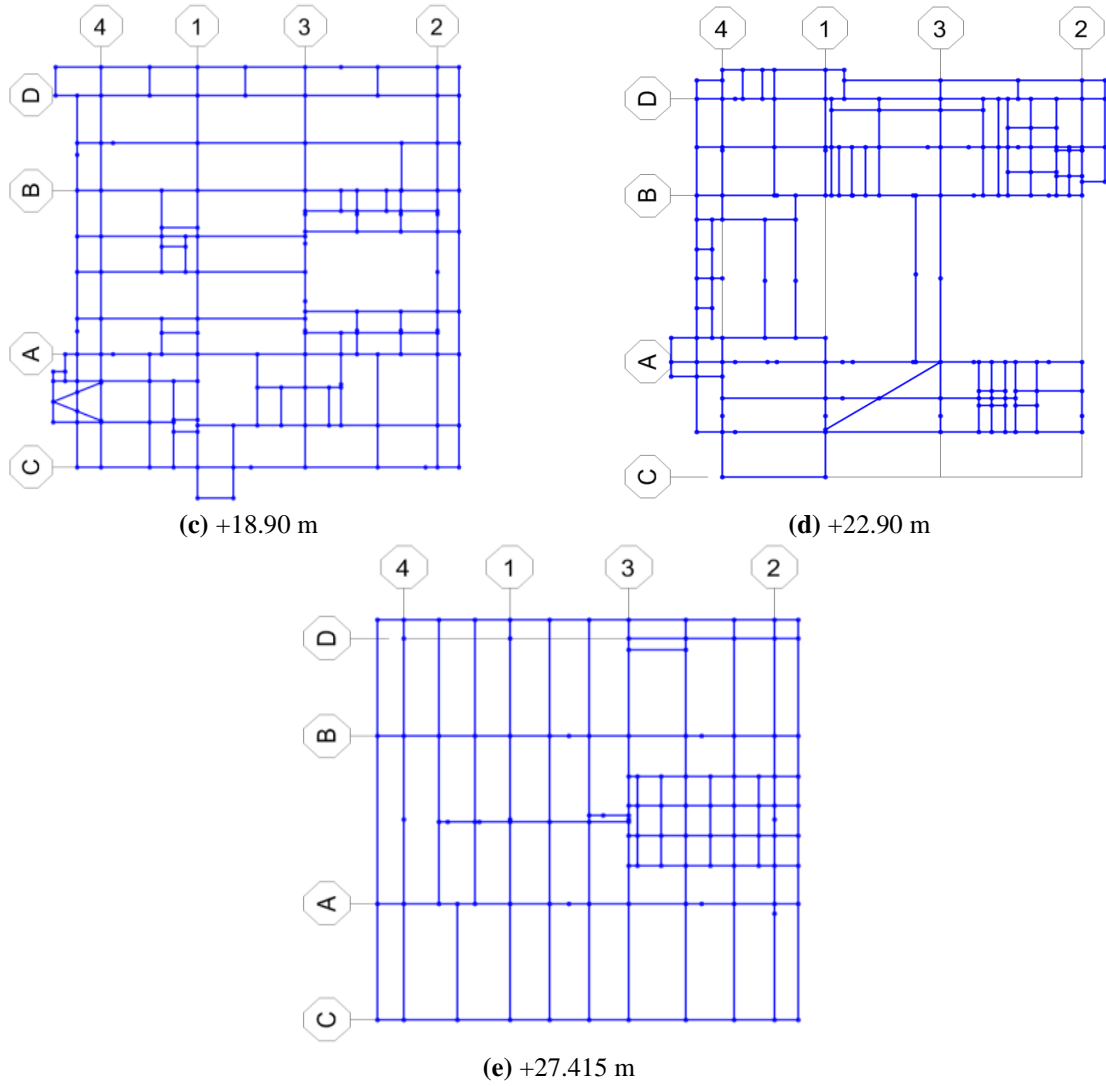
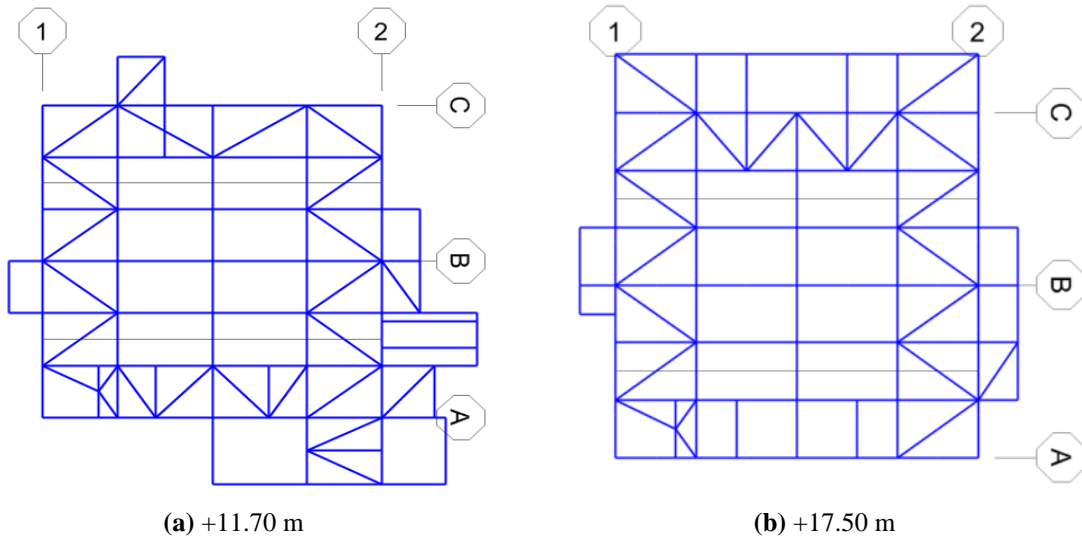
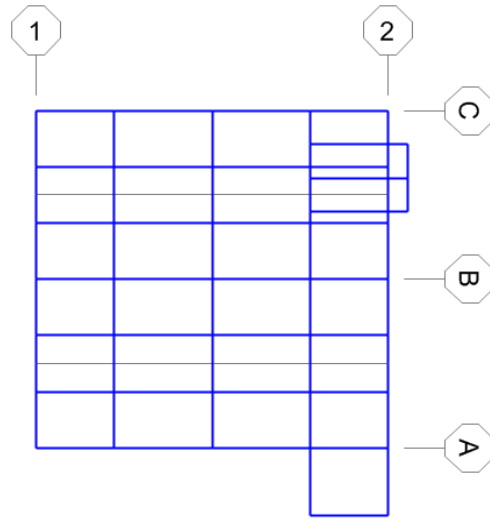


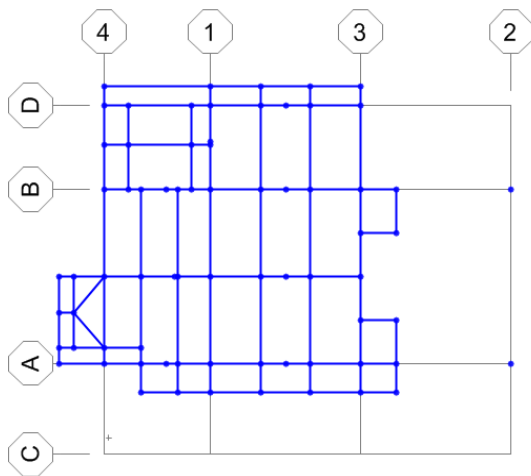
Fig. 2. Plan at the different elevations for platform No. 1



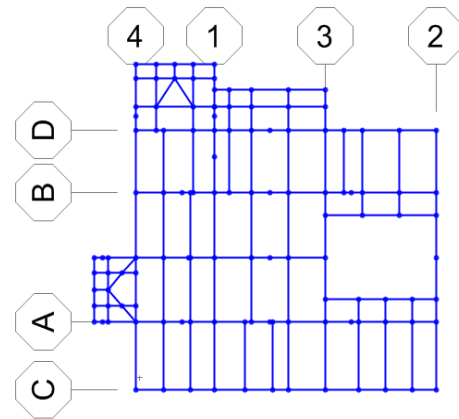


(c) +23.50 m

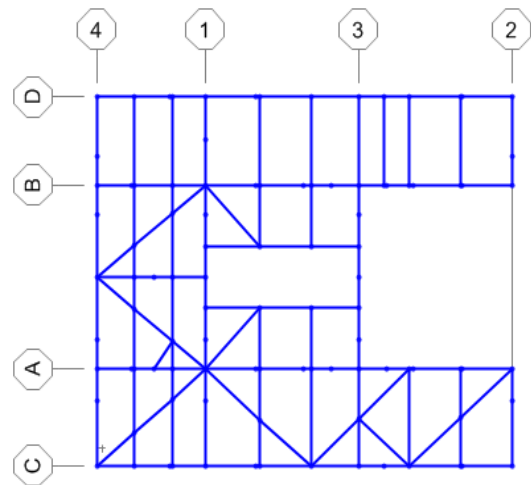
Fig. 3. Plan at the different elevations for platform No. 2



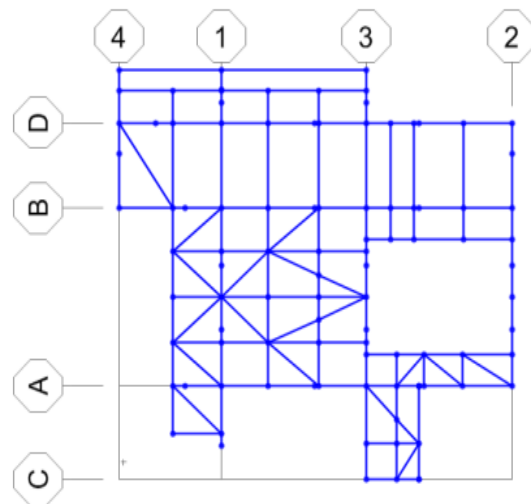
(a) +10.10 m



(b) +14.25 m



(c) +18.30 m



(d) +21.85 m

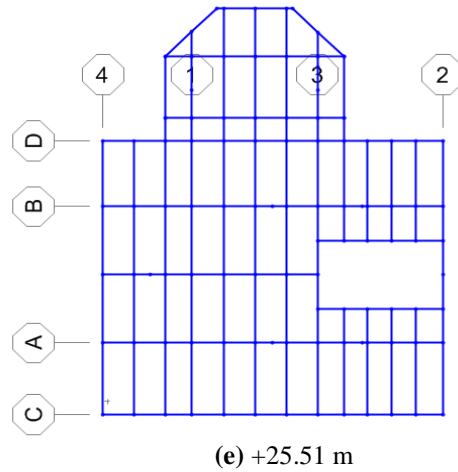


Fig. 4. Plan at the different elevations for platform No. 3

Table 1. The specifications of modeled platforms

Platform No.	Water Depth (m)	Total Height (m)	Min. Elevation	Max. Elevation	Number of Nodes	Number of Elements	Topside Weight+ Attachments (ton)	Jacket Weight (ton)	Period (sec)
1	72	99	-69.60	+27.41	1404	2224	1800	2260	1.37
2	71	94	-68.50	+23.50	356	716	5950	3700	1.91
3	63.5	89	-61.6	+25.51	646	1290	2600	1600	1.35

MODELING OF THE MATERIALS

The present study utilizes the model of stl-mp steel materials. The uniaxial stress-strain constitutive relations used for stl-mp are the commonly-used Menegotto-Pinto (1973) nonlinear hysteretic model. Figure 5 shows the steel stress-strain

diagram based on the abovementioned model. The model is computationally efficient and agrees very well with the experimental results from cyclic tests on reinforcing steel bars. The model, as presented in Menegotto and Pinto (Taucer et al., 1991) takes the following form:

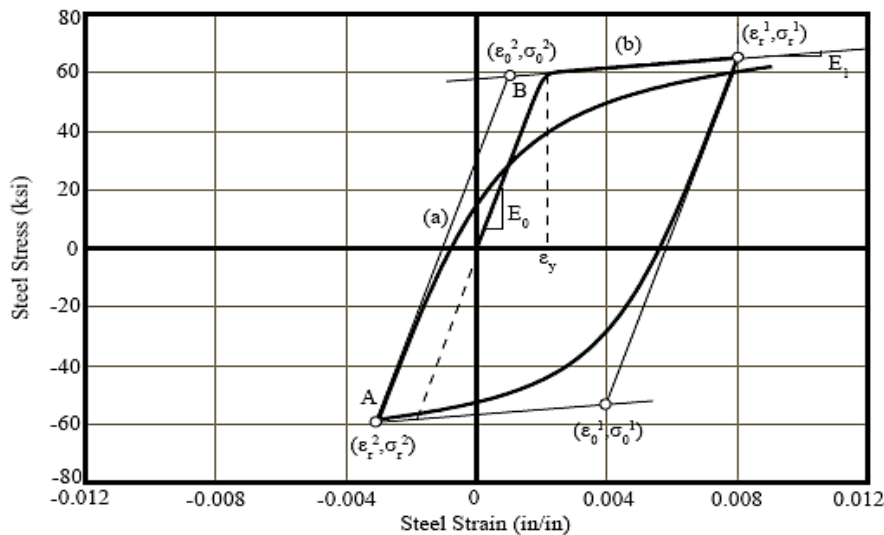


Fig. 5. Specified model for steel (Menegotto and Pinto, 1973)

$$\sigma^* = b\varepsilon^* + \frac{(1 - b)\varepsilon^*}{(1 + \varepsilon^{*R})^{\frac{1}{R}}} \quad (1)$$

where

$$\varepsilon^* = \frac{\varepsilon - \varepsilon_r}{\varepsilon_0 - \varepsilon_r} \quad (2)$$

and

$$\sigma^* = \frac{\sigma - \sigma_r}{\sigma_0 - \sigma_r} \quad (3)$$

Eq. (1) represents a curved transition from a straight line asymptote with slope E_0 to another asymptote having slope E_1 (lines (a) and (b), respectively, in Figure 5). σ_0 and ε_0 are the stress and the strain at the point where the two asymptotes of the branch under consideration meet (point B in Figure 5). Similarly, σ_r and ε_r are the stress and the strain at the point where the last strain reversal with stress of equal sign occur (point A in Figure 5); b is the strain hardening ratio, that is the ratio between slope E_1 and E_0 and R is a parameter influencing the shape of transition curve allowing suitable representation of the Bauschinger effect. As indicated in Figure 5, $(\varepsilon_0, \sigma_0)$ and $(\varepsilon_r, \sigma_r)$ are updated after each strain reversal (Taucer

et al., 1991). R is considered to be dependent on the strain difference between the current asymptote intersection point (point A in Figure 6) and the previous load reversal point with maximum or minimum strain depending on whether the corresponding steel stress is positive or negative (point B in Figure 6). The expression for R takes the form suggested by Menegotto and Pinto (Taucer et al., 1991):

$$R = R_0 - \frac{a_1 \xi}{a_2 + \xi} \quad (4)$$

where ξ : is updated following a strain reversal. R_0 : represents the value of the parameter R during initial loading and a_1, a_2 : are experimentally determined parameters to be defined together with R_0 . The definition of ξ remains valid if reloading occurs after partial unloading (Taucer et al., 1991).

ELEMENTS

Displacement-Based Nonlinear Elements (Infrmdb)

The beam-column three-dimensional element is used for modeling the members of the space frame with nonlinear properties of geometry – materials (Seissoft, 2013).

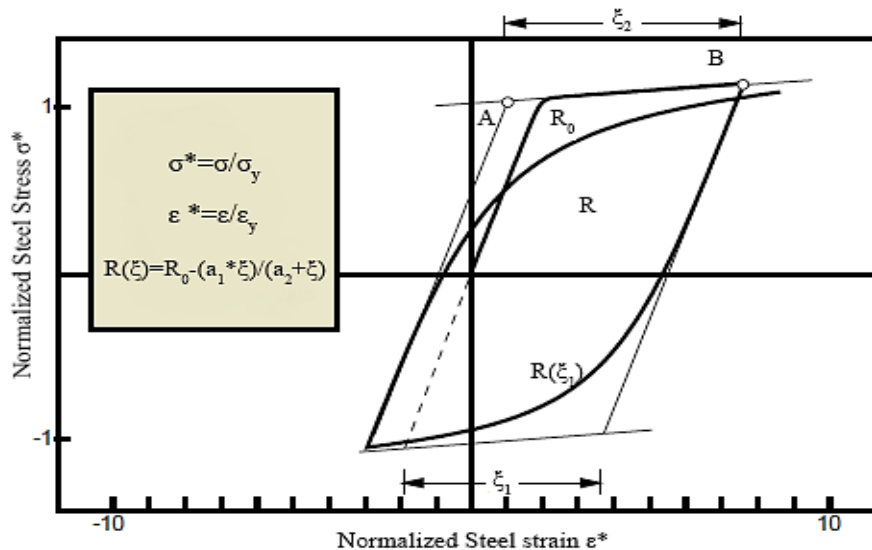


Fig. 6. Definition of curvature parameter R in Menegotto-Pinto steel model (Taucer et al., 1991)

Distributed plasticity models (DPM) which contains Force-based element (FBE) and Displacement-based element (DBE) expand plasticity along element unlike elastic element with rotational springs at element end which called concentrated plasticity models and also yielding occur at any location along element at the same time distributed loads applied on element (girders with high gravity loads) (Terzic, 2011).

Link Elements

Link elements are three-dimensional elements that can show all three operation types of bending, shear and axial action. These elements are used to connect different other elements to each other. For example, to connect a beam to a column in a structure, a link element can defined at the connection of beam and column. Using the link elements, the rigid and pinned connections of beam-column, energy-absorbing devices, and foundation ductility can be modeled. Link elements connect two matching nodes of two different elements and thus a force-displacement or moment-rotation curve needs to be defined for each of their 6 degrees of freedom (Seismosoft, 2013).

NONLINEAR INCREMENTAL DYNAMICAL ANALYSIS

One of the most recent methods for structural analysis is the Incremental Dynamic Analysis (IDA). This parametric analysis has been based on nonlinear dynamic analysis and developed to evaluate the structural performance under earthquake loads. In this method of analysis, one or more accelerograms are scaled at several levels of intensity, and are applied to the damage. Scaling the records aims at more detailed coverage of the entire range of structural behavior from the elastic state to the ultimate failure state. At each step of scaling, the structural model is analyzed under the desired

records and one or more curves of the damage response versus intensity are achieved. Using these curves, the limiting states can be defined synthesizing the results with the curve of probable analyses assessing the structures. The unique information that this curve provides about the response of structures with several degrees of freedom explains the widespread use of this method. Nevertheless, this process is difficult and time consuming (Jalayer and Cornell, 2000). The results of nonlinear incremental dynamic analysis are drawn as cluster curves.

In the present study, the vertical axis of these curves represents the intensity in terms of spectral acceleration parameter in the structure vibration dominant mode with regard to 5% ($S_a(T1,5\%)$) damping and the horizontal axis represents the measure of the damage with the maximum floor drift parameter (Θ_{max}).

SELECTION OF ACCELEROGRAMS

Previous research has shown that 10 to 20 records of earthquake usually provide adequate accuracy to estimate the seismic demand for structures (Vamvatsikos and Cornell, 2002). In order to evaluate the seismic features of the studied structures, 14 accelerograms scaled with relatively large magnitude (6.5-6.9) and balanced distance related with the horizontal component of the earthquakes were used. All these accelerograms were related to soil type 2 obtained from the PEER site. The selected accelerograms are assumed to be representative of possible events that cause severe earthquake in the site where structures are located (Asgarian et al., 2010). Characteristics of the accelerograms are given in Table 2. According to the criterion of API Code (RP 2A-WSD) (American Petroleum Institute, 2000) accelerograms have to be simultaneously applied to structures in three directions. The values of

accelerograms in the horizontal directions (X and Y) are equal and the value of accelerograms in the vertical direction (Z) is considered as being 50% of the value of the horizontal directions (American Petroleum Institute, 2000). The cluster curves are plotted for both directions of X and Y, then the curve of each direction, which reaches faster to relative displacement (0.1) that is corresponding to the performance state of the collapse prevention (according to FEMA355-F guidelines), is used in the calculations.

RESULTS OF THE IDA

Cluster Curves

In this section, the results of incremental nonlinear dynamic analysis are presented as

cluster curves for the 14 applied accelerograms and a summary of IDA curves is presented. Figures 7 to 12 show the cluster curves of the platforms studied. Examining the above curves, it is observed that platforms 1 and 3 behave in the same manner which is due to the geometric similarity between the two, and the maximum relative displacement between floors is nearly the same. Almost in none of the curves related to these structures, even at high spectral accelerations, global dynamic instability (curve slope of zero) occurs and the slope of the elastic part is almost identical. However, the curves related to platform number 2 reveal differences that are mainly due to its very different geometry as compared with the other platforms.

Table 2. The characteristics of accelerograms used in the dynamic time history analysis (Asgarian et al., 2010)

No	ID	Event	Station	ϕ^{o1}	Soil ²	M ³	R ⁴ (km)	PGA (g)
1	NR1	Northridge, 1994	24 278 Castaic-Old Route	90	B, B	6.7	22.6	0.568
2	NR2	Northridge, 1994	14 403 LA-116th St School	90	B, D	6.7	41.9	0.208
3	NR3	Northridge, 1994	24 396 Malibu-Point DumeSch	90	B, B	6.7	35.2	0.13
4	NR4	Northridge, 1994	24 400 LA-Obregon Park	90	B, D	6.7	37.9	0.355
5	SF1	San Fernando, 1971	262 Palmdale Fire Station	21	B, D	6.6	25.4	0.151
6	SF2	San Fernando, 1971	80 053 Pasadena-CIT Athenaeum	0	B, D	6.6	31.7	0.088
7	SF3	San Fernando, 1971	287 Upland-San Antonio Dam	15	B, A	6.6	58.1	0.058
8	SF4	San Fernando, 1971	290 Wrightwood-6074 Park Dr	25	B, B	6.6	60.3	0.061
9	IV1	Imperial Valley, 1979	6604 Cerro Prieto	14	B, A	6.5	26.5	0.169
10	LP1	Loma Prieta, 1989	57 064 Fremont-Mission San Jose	0	B, B	6.9	43	0.124
11	NR5	Northridge, 1994	14 196 Inglewood-Union Oil	0	B, D	6.7	44.7	0.091
12	LP3	Loma Prieta, 1989	58 262 Belmont- Envirotech	0	B, A	6.9	49.9	0.108
13	LP4	Loma Prieta, 1989	58 471 Berkeley LBL	0	B, A	6.9	83.6	0.057
14	LP5	Loma Prieta, 1989	1678 Golden Gate Bridge	27	B, A	6.9	85.1	0.233

1 Component

2 USGS, Geomatrix soil class

3 Moment magnitude

4 Closest distance to fault rupture

Slope of the elastic part of platform number 2 is slightly higher than the other two platforms, and the average relative displacement between the floors of the platform number 2 is larger than the other two platforms which could be due to its heavier weight in comparison to the other two platforms. However, the three platforms are similar in that in all platforms, the maximum relative displacement between the floors in the low spectral acceleration reaches the collapse prevention state (CP), (0.1).

Accordingly, the behavior of platforms to the point of reaching the performance level of collapse prevention is almost linear. Nevertheless, it seems that the above phenomenon occurs due to the application of records in three directions simultaneously. If the records were to be applied only in one direction only, the relative displacement should have decreased significantly. The result from applying accelerograms only in the direction X for platform number 1 (with rigid connections) supports this statement (Figure 13).

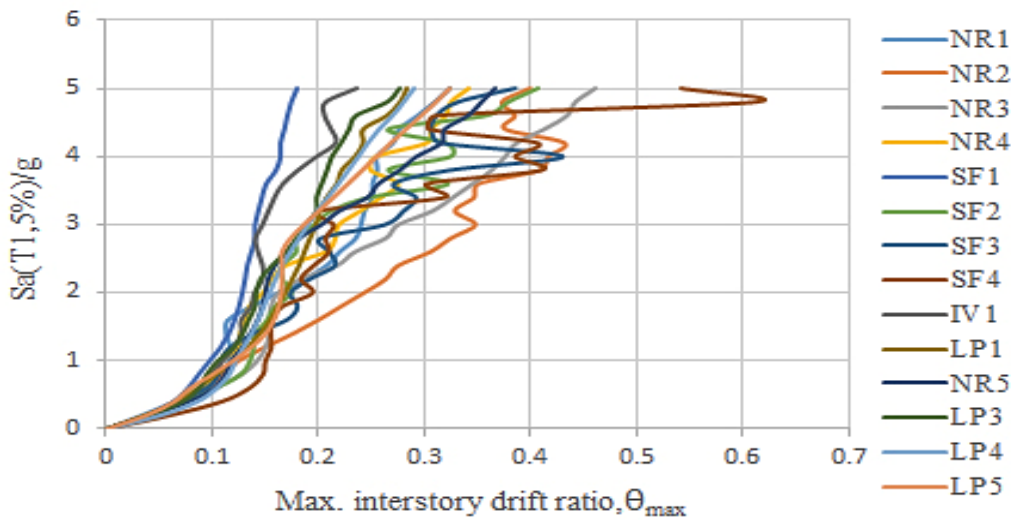


Fig. 7. Cluster curves of platform No. 1 (rigid connections)

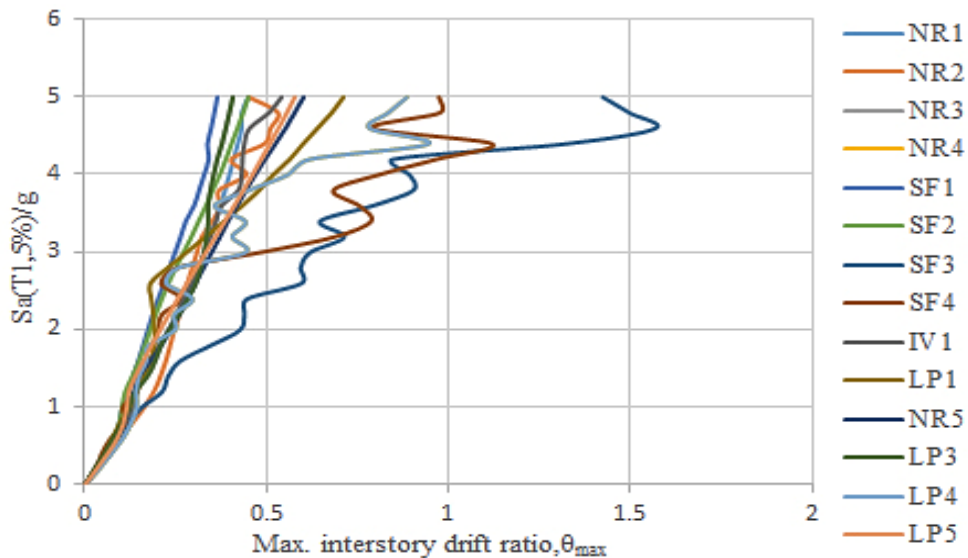


Fig. 8. Cluster curves of platform No. 2 (rigid connections)

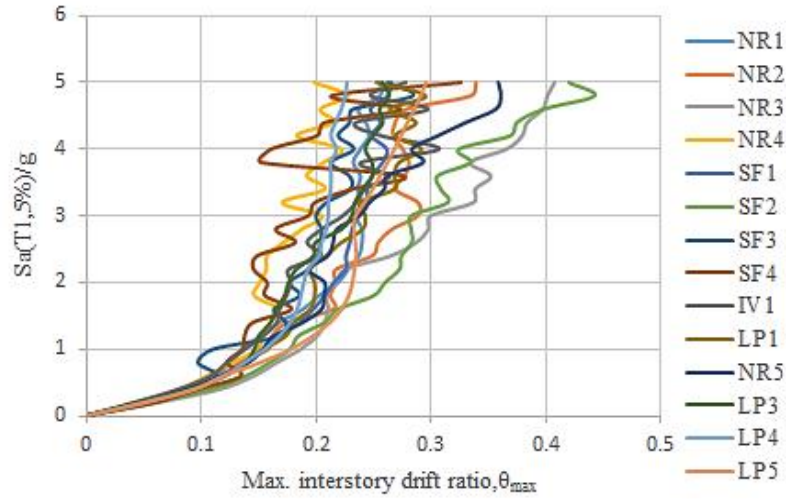


Fig. 9. Cluster curves of platform No. 3 (rigid connections)

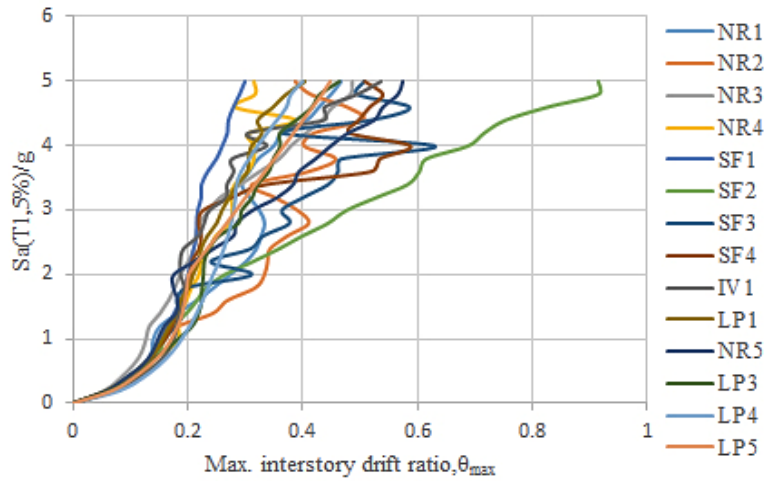


Fig. 10. Cluster curves of platform No. 1 (pinned connections)

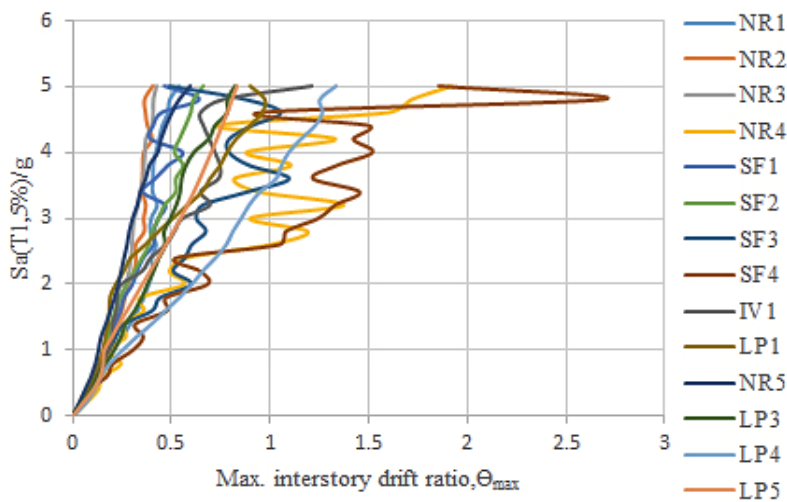


Fig. 11. Cluster curves of platform No. 2 (pinned connections)

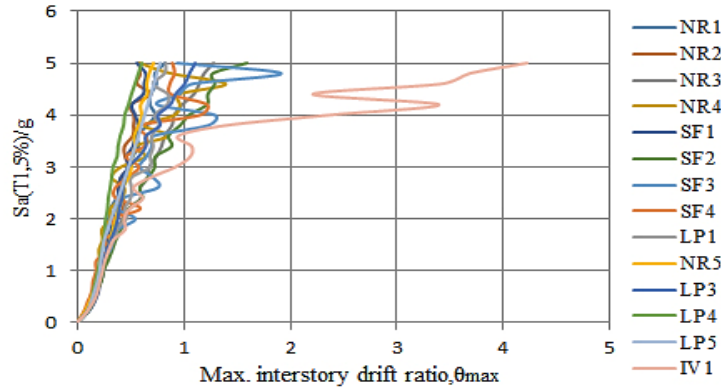


Fig. 12. Cluster curves of platform No. 3 (pinned connections)

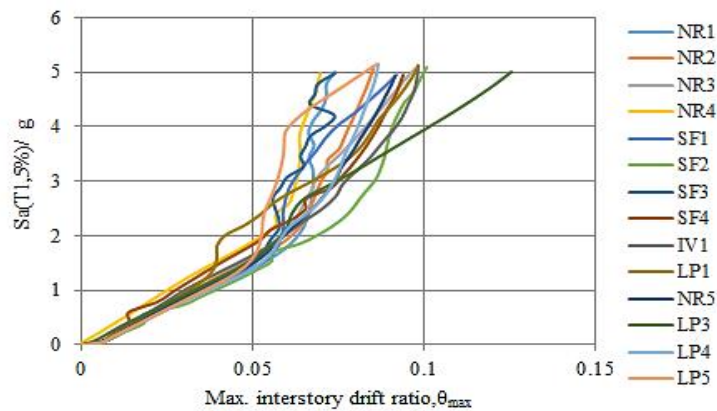


Fig. 13. Cluster curves of platform No. 1, (the result of applying accelerograms only in the X direction)

Summary of the IDA Curves

Figures 14 through 16 show the summary of IDA curves (16%, 50% and 84%) for the studied structures. Comparing the curves of platforms with rigid connections and platforms with pinned connections reveals that in the case of pinned connections, structures reach the collapse prevention state at lower spectral accelerations. In this case, the average drift between the floors is also higher which indicates the softer behavior in contrast to the rigid connections.

RELIABILITY ANALYSIS

In this study, to evaluate the seismic performance, a structure based seismic reliability has been used. To quantify the reliability, three parameters have been defined that are expressed by the probabilistic

concepts (Bertero, 2002). The first one is the intensity of ground motion, which is shown using a level of spectral acceleration for the natural period of vibration of the structure in the dominant mode considering the damping ratio of 5%, the second one is the displacement demand for the structure (D) and the third one is displacement capacity of the structure (C) (Hamburger and Moehle, 2002). Based on the FEMA guidelines, an efficient method has been developed to assess the confidence level where the structure satisfies the objectives of the project, i.e. to achieve a 95% confidence level where a structure reaches the performance level of global collapse prevention under severe earthquakes (Figure 17), (with the possibility of 2% in 50 years). For this purpose, according to FEMA 355-F guidelines, the confidence factor is initially calculated using the following equation:

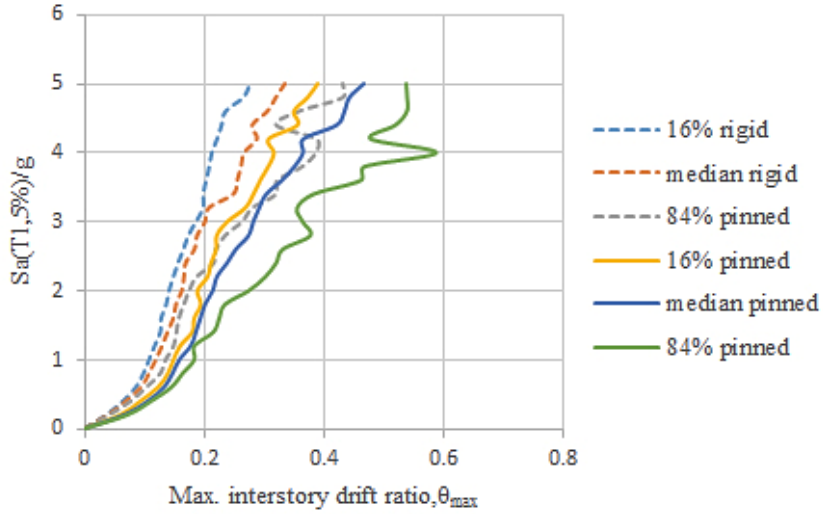


Fig. 14. Comparison of summary of IDA curves for models with rigid and pinned connections (platform No. 1)

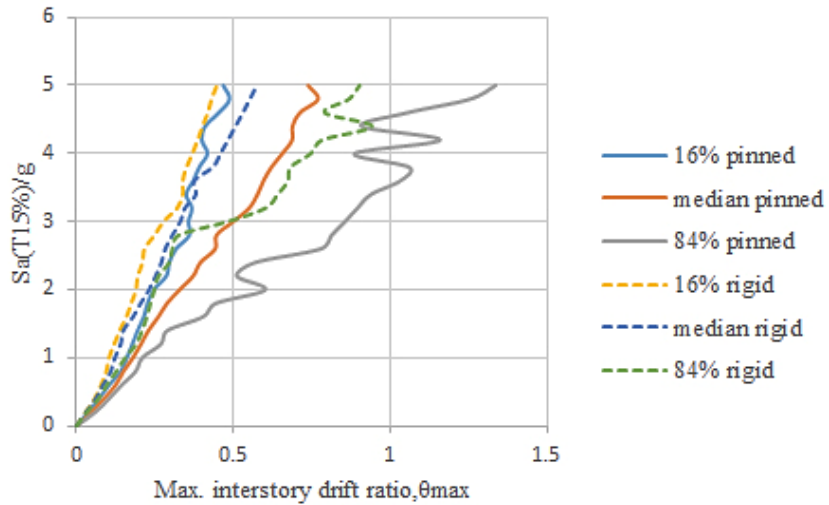


Fig. 15. Comparison of summary of IDA curves for models with rigid and pinned connections (platform No. 2)

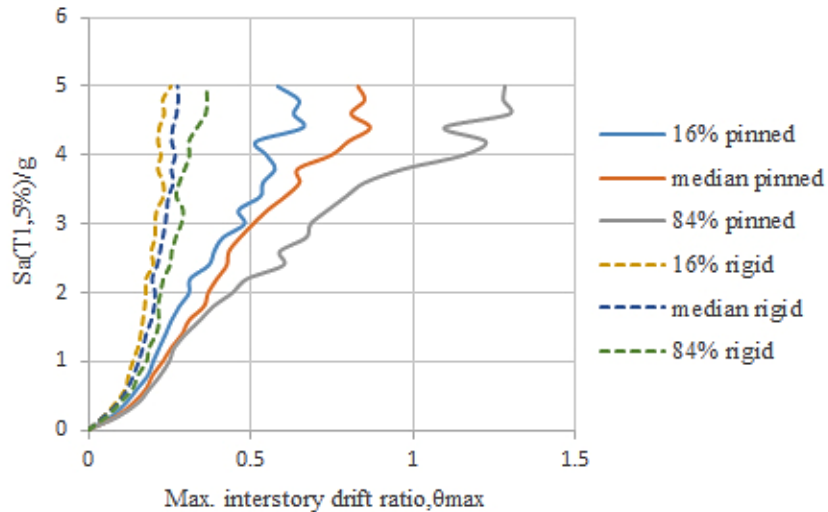


Fig. 16. Comparison of summary of IDA curves for models with rigid and pinned connections (platform No. 3)

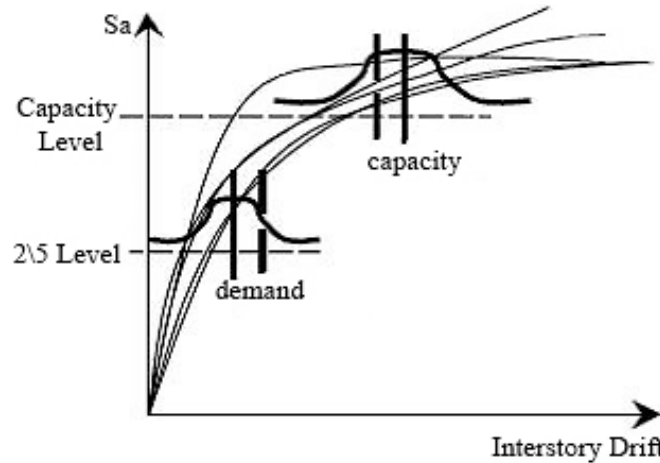


Fig. 17. The method of determination of displacement demand from IDA curves (FEMA, 2000)

$$\lambda = \frac{\phi \hat{C}}{\gamma \gamma_a \hat{D}} \quad (5)$$

where \hat{D} : is the median demand estimate, \hat{C} : is the median capacity estimate, ϕ : represents the resistance factor, γ : is the demand factor, γ_a : is the analysis demand factor and λ : is the confidence factor which determines the confidence level (Federal Emergency Management Agency, 2000).

Determination of Relative Displacement Capacity, \hat{C} :

Relative displacement capacity is determined based on global collapse. (0.1)

Determination of Resistance Factor ϕ :

Resistance factor ϕ includes the effects of uncertainties and randomness in the estimation process of \hat{C} . Eqs. (6) to (8) have been provided by Cornell et al. to determine ϕ (Kim et al., 2004):

$$\phi = \phi_{RC} \cdot \phi_{UC} \quad (6)$$

$$\phi_{RC} = e^{\frac{-k \beta_{RC}^2}{2b}} \quad (7)$$

$$\phi_{UC} = e^{\frac{-k \beta_{UC}^2}{2b}} \quad (8)$$

where ϕ : is resistance factor, ϕ_{RC} : contribution to ϕ from randomness of the earthquake accelerograms, ϕ_{UC} :

Contribution to ϕ from uncertainties in measured capacity, β_{RC} : is standard deviation of the natural logarithm of the relative displacement capacity of IDA analysis, β_{UC} : is dependent part of demand capacity, k : is slope of the hazard curve and b : depends on the level of variation in the capacity compared to variation in the demand. As suggested by FEMA, b is considered equal to 1.

Local Variations of the Slope of the Hazard Curve, k

The slope of the hazard curve, k , is a function of the hazard level, location of the structure (in hazard zone), and the period. The hazard curve is a plot of the annual exceedance probability versus the spectral acceleration in log-log scale. According to Eq. (9) the hazard levels of 2% in 50 years and 10% in 50 years are used in the present study to calculate the slope of the curve and the parameter k .

$$k = \frac{\ln \left[\frac{H_{Sa10\%}}{H_{Sa2\%}} \right]}{\ln \left[\frac{Sa_{2\%}}{Sa_{10\%}} \right]} \quad (9)$$

Determination of β_{RC}

β_{RC} is natural logarithm standard deviation of drift capacity that is obtained according to Table 4.

Table 3. Calculated K parameter (the slope of the hazard curve) for the modeled platforms

Model	Model 1	Model 1	Model 2	Model 2	Model 3	Model 3
	Rigid Connections	Pinned Connections	Rigid Connections	Pinned Connections	Rigid Connections	Pinned Connections
Period(s)	1.37	1.48	1.91	2.15	1.35	1.63
K	2.04	2.00	2.10	2.39	2.04	1.96

Sa_{10%} = Spectral amplitude for the hazard level of 10% in 50 years

Sa_{2%} = Spectral amplitude for the hazard level of 2% in 50 years

H_{Sa} (Sa_{10%}) = Exceedance probability for 10% in 50 years, which is equal to 1/475=0.0021

H_{Sa} (Sa_{2%}) = Exceedance probability for 2% in 50 years, which is equal to 1/2475=0.00040. In this study, the zone hazard spectra shown in Figure 18.

Table 4. Calculated drift capacity and β_{RC} for global collapse (all platforms)

	All models	
	Max. Drift	LN()
NR1	0.1000	-2.3026
NR2	0.1000	-2.3026
NR3	0.1000	-2.3026
NR4	0.1000	-2.3026
SF1	0.1000	-2.3026
SF2	0.1000	-2.3026
SF3	0.1000	-2.3026
SF4	0.1000	-2.3026
IV	0.1000	-2.3026
LP1	0.1000	-2.3026
NR5	0.1000	-2.3026
LP3	0.1000	-2.3026
LP4	0.1000	-2.3026
LP5	0.1000	-2.3026
Mean (LN)		-2.3026
Median	\hat{C}	0.1000
STD (LN)	β_{RC}	0

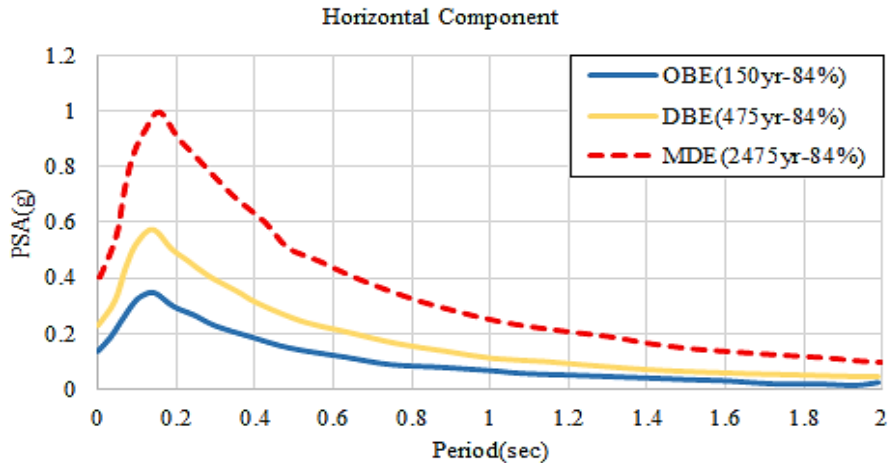


Fig. 18. Uniform hazard spectra of the desired site (Soleimani and Nurzad, 2012)

Determination of β_{UC}

The above parameter is determined based on Eq. (10):

$$\beta_{UC} = \sqrt{3} \cdot \beta_{NTH} \quad (10)$$

where β_{NTH} : is associated with the uncertainties in the non-linear time history analysis method. In the SAC (A partnership of Structural Engineers Association of California (SEAOC), Applied Technology Council (ATC), California Universities for Research in Earthquake Engineering (CUREE)) project, β_{NTH} parameter for 3, 9 and 20 stories buildings is 0.15, 0.20 and 0.25, respectively (Soleimani and Nurzad, 2012). In this study, β_{NTH} value of 0.25, is considered due to the closeness of the structures height with the 20-stories building of group SAC. Therefore, according to Equation 6, β_{UC} value of 0.43 is obtained. Now, after the calculation of the above parameters, resistance factor can be calculated according to Table 5.

Determination of the Demand Factor γ

Demand factor is associated with the randomness property caused by the accelerograms of earthquake and the orientation of the building with respect to the fault axis and is calculated according to Eqs. (11) and (12):

$$\gamma = e^{\frac{k \beta_{RD}^2}{2b}} \quad (11)$$

$$\beta_{RD} = \sqrt{\beta_{or}^2 + \beta_{acc}^2} \quad (12)$$

where β_{or} (randomness): is caused by the orientation of the building with respect to the fault axis. Considering the use of records, which are far from fault and independent of direction, this parameter is not considered in the assessment process.

Determination of β_{acc}

The standard deviation of the natural logarithm of the drift demand (β_{acc}) and drift demand (\hat{D}) for different platforms have been shown in Tables 6 to 8. With these values, the demand factor is obtained for different

models according to Table 9.

Determination of the Analysis Demand factor γ_a

The analysis demand factor γ_a based on uncertainties related to demand, \hat{D} , is determined using the Eqs. (13) and (14).

$$\gamma_a = e^{\frac{k \beta_{UD}^2}{2b}} \quad (13)$$

$$\beta_{UD} = \sqrt{\beta_i^2} \quad (14)$$

The parameter β , which is caused by uncertainty, is a combination of several parts. β_{NTH} : is associated with the uncertainty in the non-linear time history analysis method that has been described previously, $\beta_{damping}$: is associated with the uncertainty in the estimation of structure's damping, β_{period} : is associated with uncertainty in the period of structure and $\beta_{material}$: is associated with uncertainty in properties of materials. Values of the uncertainty factors related to damping, periods and materials are very small and have been calculated previously by Kim et al. (2004). Accordingly, the values for the above factors have been considered in Table 10 and the values of analysis demand factor are calculated using Eqs. (13) and (14).

Determination of the Total Uncertainty Factor

To calculate the total uncertainty, Eq. (15) is used. β_{UC} is related to the capacity part, and β_{UD} is related to the demand part which is equal to 0.43 as calculated in previous section. β_{UD} is the second root of the sum of squares of β obtained from uncertainties in the process of analysis that as presented in Table 10 and its value for all models is equal to 0.27. The total uncertainty factor for the global collapse of platforms in all models has been identical and is obtained from Table 11.

$$\beta_{UT} = \sqrt{(\beta_{UC}^2 + \beta_{UD}^2)} \quad (15)$$

Table 5. Calculated resistance factors for the global collapse of platforms

	β_{RC}	Φ_{RC}	β_{UC}	Φ_{UC}	Φ
Model 1-rigid connections	0	1.00	0.43	0.83	0.83
Model 1-pinned connections	0	1.00	0.43	0.79	0.79
Model 2-rigid connections	0	1.00	0.43	0.82	0.82
Model 2-pinned connections	0	1.00	0.43	0.80	0.80
Model 3-rigid connections	0	1.00	0.43	0.83	0.83
Model 3-pinned connections	0	1.00	0.43	0.83	0.83

Table 6. Median drift demand and β_{acc} for global collapse of Platform No. 1

	Model 1 - Rigid Connections		Model 1 - Pinned Connections	
	Max. Drift	LN()	Max. Drift	LN()
NR1	0.029844	-3.51178	0.048593	-3.02428
NR2	0.033957	-3.38265	0.048727	-3.02153
NR3	0.037305	-3.28863	0.043989	-3.12381
NR4	0.03303	-3.41034	0.057467	-2.85655
SF1	0.033135	-3.40715	0.053161	-2.93443
SF2	0.037242	-3.29033	0.052539	-2.9462
SF3	0.035042	-3.3512	0.054979	-2.90081
SF4	0.053247	-2.93281	0.054769	-2.90464
IV	0.033511	-3.39589	0.057777	-2.85117
LP1	0.032972	-3.41208	0.046948	-3.05871
NR5	0.036632	-3.30683	0.047416	-3.0488
LP3	0.035847	-3.3285	0.052098	-2.95463
LP4	0.045751	-3.08454	0.064945	-2.73422
LP5	0.033496	-3.39633	0.054955	-2.90124
Mean (LN)		-3.32136		-2.94722
Median	\hat{D}	0.0345	\hat{D}	0.05285
STD (LN)	β_{acc}	0.148	β_{acc}	0.102

Table 7. Median drift demand and β_{acc} for global collapse of Platform No. 2

	Model 2-rigid Connections		Model 2-pinned Connections	
	Max. Drift	LN()	Max. Drift	LN()
NR1	0.017206	-4.06247	0.020267	-3.8987693
NR2	0.016601	-4.0983	0.017787	-4.0292976
NR3	0.014216	-4.2534	0.015015	-4.1986859
NR4	0.02125	-3.8514	0.026774	-3.6203125
SF1	0.015524	-4.1654	0.02356	-3.7482044
SF2	0.016398	-4.11057	0.017348	-4.05428
SF3	0.016021	-4.13386	0.01941	-3.9419549
SF4	0.015899	-4.1415	0.018399	-3.9954372
IV	0.017789	-4.02915	0.019303	-3.9474826
LP1	0.016626	-4.09681	0.014969	-4.2017419
NR5	0.017025	-4.07305	0.013187	-4.3285207
LP3	0.016429	-4.10872	0.018538	-3.9879305
LP4	0.022694	-3.78564	0.0262	-3.6419908
LP5	0.017086	-4.0695	0.020106	-3.9067447
Mean (LN)		-4.06998		-3.9643824
Median	\hat{D}	0.016613	\hat{D}	0.018921
STD (LN)	β_{acc}	0.120	β_{acc}	0.203

Calculation of the Confidence Factors and Levels

Finally, the confidence factors can be calculated using the above calculated

parameters from Eq. (5). With specified confidence factor (λ), the uncertainty factor (β_{UT}), and the slope of the hazard curve (k), confidence levels are obtained from Table 12

(FEMA, 2000). All confidence levels calculated for platforms with rigid connections exceed 95%. As can be seen in this table, confidence level of rigid model 3 is slightly less than those of the other two rigid models which is because of the higher median demand. According to Eq. (1) this leads to lower confidence coefficient and a lower confidence level. However, among platforms with pinned connections, only the confidence level for platform number 2 achieved a value higher than 95% and the other two platforms could not provide the desired confidence level of FEMA for the performance level of

collapse prevention .The high confidence level of platform number 2 is due to the specific geometry of this platform that gives it a higher period in comparison to the other models; in addition considering the area uniform hazard spectra curve, spectral acceleration corresponding to the hazard level of 2% in 50 years for this platform represents a small value and consequently the median demand corresponding to this spectral acceleration is also small leading to a higher confidence factor and a higher confidence level.

Table 8. Median drift demand and β_{acc} for global collapse of platform No. 3

	Model 3 - Rigid Connections		Model 3 - Pinned Connections	
	Max. Drift	LN()	Max. Drift	LN()
NR1	0.046891	-3.05993	0.058479	-2.83908
NR2	0.051914	-2.95817	0.050178	-2.99218
NR3	0.057616	-2.85396	0.050809	-2.97967
NR4	0.039735	-3.22553	0.060115	-2.81149
SF1	0.043192	-3.1421	0.07084	-2.64733
SF2	0.053977	-2.91921	0.067829	-2.69077
SF3	0.044564	-3.11084	0.060525	-2.8047
SF4	0.055394	-2.89329	0.043683	-3.13079
IV	0.038846	-3.24814	0.062845	-2.76709
LP1	0.043303	-3.13954	0.065149	-2.73107
NR5	0.043382	-3.13771	0.048116	-3.03415
LP3	0.044743	-3.10683	0.05995	-2.81424
LP4	0.045363	-3.09305	0.062695	-2.76948
LP5	0.048343	-3.02943	0.0647	-2.738
Mean (LN)		-3.06555		-2.83929
Median	\bar{D}	0.045053	\bar{D}	0.06032
STD (LN)	β_{acc}	0.120	β_{acc}	0.141

Table 9. The calculated demand factors for global collapse of platforms

	β_{acc}	β_{RD}	γ
Model 1-rigid connections	0.148	0.148	1.02
Model 1-pinned connections	0.102	0.102	1.01
Model 2-rigid connections	0.120	0.120	1.02
Model 2-pinned connections	0.203	0.203	1.05
Model 3-rigid connections	0.120	0.120	1.01
Model 3-pinned connections	0.141	0.141	1.02

Table 10. The calculated analysis demand factors for global collapse of platforms

	β_{NTH}	$\beta_{damping}$	β_{period}	$\beta_{material}$	β_{UD}	γ_a
All models	0.25	0.08	0.01	0.08	0.27	1.08

Table 11. The calculated total uncertainty factor for global collapse of platforms

	β_{UC}	β_{UD}	β_{UT}
All models	0.43	0.27	0.51

CALCULATION OF THE PROBABILITY OF THE STRUCTURE EXCEEDING THE PERFORMANCE LEVEL OF COLLAPSE PREVENTION

According to FEMA, the total probability theory can be used to evaluate the performance of steel moment resisting frame systems. The total probability of failure in mathematics is defined as follows (Jalayer and Cornell, 2000):

$$P_{PL} = P(C \leq D) = \int P(C \leq D | D = d_i) | dH_D(d) | \quad (16)$$

where P_{PL} : is the probability of failure or the probability of exceeding the desired performance level, and $P(C \leq D | D = d_i)$: is the conditional probability of structural failure with respect to the specific intensity (d_i) of the earthquake that the structure will experience. $| dH_D(d) |$: is the absolute value of derivative of the average function of the area risk (Hamburger and Moehle, 2002). The probability of not achieving the desired performance level can be calculated by the integration of Eq. (16) and using the risk function of average displacement:

$$P_{PL} = H(S_a^{\hat{c}}) \exp \left[\frac{1}{2} \frac{k^2}{b^2} (\beta_{Dis_a}^2 + \beta_C^2) \right] \quad (17)$$

where $S_a^{\hat{c}}$: represents the spectral acceleration of the median capacity of displacement, a level of spectral acceleration, which presents a displacement demand equal to the median drift capacity \hat{C} in the structure (Jalayer and

Cornell, 2000). The distribution curve of displacement demand is assumed as a normal log and has a logarithmic standard deviation β_{Dis_a} . These assumptions are also considered about the displacement capacity where logarithmic standard deviation is considered β_C (Jalayer and Cornell, 2000). Now, the annual exceedance probability can be calculated through Poisson's formula.

$$P(t) = 1 - e^{(-P_{PL} \times t)} \quad (18)$$

where $P(t)$: is the exceedance probability of the desired performance level at the time of t .

Calculation of β_C

The above parameter is obtained from Eq. (19):

$$\beta_C = \sqrt{(\beta_{UC}^2 + \beta_{RC}^2)} \quad (19)$$

As β_{UC} and β_{RC} factors have been determined in the previous section, the value of β_C for all models can be found in Table 14.

Calculation of β_D

For this purpose, Eq. (20) is used:

$$\beta_D = \sqrt{(\beta_{UD}^2 + \beta_{RD}^2)} \quad (20)$$

As β_{UD} and β_{RD} factors have been determined in the previous section, the value of β_D for all models can be found with reference to Table 15.

Now, the probability of exceeding the performance level of collapse prevention can be calculated using Eqs. (13) and (14), (Table 16).

Table 12. λ as a function of confidence level, hazard level parameter k, and uncertainty β_{UT} (FEMA, 2000)

Confidence	2%	5%	10%	20%	30%	40%	50%	60%	70%	80%	90%	95%	98%
$\beta_{UT} = 0.3$													
k = 1	0.52	0.58	0.7	0.7	0.82	0.89	1	1.03	1.12	1.23	1.4	1.57	1.77
k = 2	0.49	0.56	0.6	0.7	0.78	0.85	0.9	0.99	1.07	1.18	1.34	1.5	1.69
k = 3	0.47	0.53	0.6	0.7	0.75	0.81	0.9	0.94	1.02	1.12	1.28	1.43	1.62
k = 4	0.45	0.51	0.6	0.7	0.71	0.77	0.8	0.9	0.98	1.08	1.23	1.37	1.55
$\beta_{UT} = 0.4$													
k = 1	0.41	0.48	0.6	0.7	0.75	0.83	0.9	1.02	1.14	1.29	1.54	1.78	2.1
k = 2	0.37	0.44	0.5	0.6	0.69	0.77	0.9	0.94	1.05	1.19	1.42	1.65	1.94
k = 3	0.35	0.41	0.5	0.6	0.64	0.71	0.8	0.87	0.97	1.1	1.31	1.52	1.79
k = 4	0.32	0.38	0.4	0.5	0.59	0.66	0.7	0.8	0.9	1.02	1.21	1.4	1.65
$\beta_{UT} = 0.5$													
k = 1	0.32	0.39	0.5	0.6	0.68	0.78	0.9	1	1.15	1.34	1.67	2.01	2.46
k = 2	0.28	0.34	0.4	0.5	0.6	0.69	0.8	0.88	1.01	1.19	1.48	1.77	2.17
k = 3	0.25	0.3	0.4	0.5	0.53	0.61	0.7	0.78	0.89	1.05	1.3	1.56	1.92
k = 4	0.22	0.27	0.3	0.4	0.47	0.53	0.6	0.69	0.79	0.92	1.15	1.38	1.69
$\beta_{UT} = 0.6$													
k = 1	0.24	0.31	0.4	0.5	0.61	0.72	0.8	0.97	1.14	1.38	1.8	2.24	2.86
k = 2	0.2	0.26	0.3	0.4	0.51	0.6	0.7	0.81	0.96	1.16	1.51	1.87	2.39
k = 3	0.17	0.22	0.3	0.4	0.43	0.5	0.6	0.68	0.8	0.97	1.26	1.56	2
k = 4	0.14	0.18	0.2	0.3	0.36	0.42	0.5	0.57	0.67	0.81	1.05	1.31	1.67
$\beta_{UT} = 0.7$													
k = 1	0.19	0.25	0.3	0.4	0.54	0.66	0.8	0.93	1.13	1.41	1.92	2.48	3.3
k = 2	0.15	0.19	0.3	0.3	0.42	0.51	0.6	0.73	0.88	1.1	1.5	1.94	2.58
k = 3	0.11	0.15	0.2	0.3	0.33	0.4	0.5	0.57	0.69	0.86	1.18	1.52	2.02
k = 4	0.09	0.12	0.2	0.2	0.26	0.31	0.4	0.45	0.54	0.68	0.92	1.19	1.58

Table 13. Calculated confidence factors and confidence levels for global collapse of platforms

	ϕ	C	γ	γ_a	D	β_{UT}	k	λ	$C.L.*(\%)$
Model 1-rigid connections	0.83	0.1	1.02	1.08	0.0345	0.51	2.04	2.18	98
Model 1-pinned connections	0.79	0.1	1.01	1.08	0.0528	0.51	2.00	1.45	89
Model 2-rigid connections	0.82	0.1	1.02	1.08	0.0166	0.51	2.10	4.52	98
Model 2-pinned connections	0.80	0.1	1.05	1.07	0.0189	0.51	2.39	3.70	98
Model 3-rigid connections	0.83	0.1	1.01	1.08	0.0450	0.51	2.04	1.68	95
Model 3-pinned connections	0.83	0.1	1.02	1.09	0.0603	0.51	1.96	1.26	80

* Confidence level

Table 14. Logarithmic standard deviation of drift capacity

	β_{UC}	β_{RC}	β_C
All models	0.43	0	0.43

Table 15. Logarithmic standard deviation of drift demand

	β_{UD}	β_{RD}	β_D
Model 1-rigid connections	0.27	0.148	0.31
Model 1-pinned connections	0.27	0.102	0.29
Model 2-rigid connections	0.27	0.120	0.30
Model 2-pinned connections	0.27	0.203	0.34
Model 3-rigid connections	0.27	0.120	0.30
Model 3-pinned connections	0.27	0.141	0.30

Table 16. Calculation of annual exceedance probability of collapse prevention performance level

	b	k	β_D	β_C	$S_a(C)$	$H(S_a^c)$	P_{PL}	Probability of Exceedance in 50 Years (%)
Model 1-rigid connections	1.00	2.04	0.31	0.43	0.8	1E-04	1.8E-04	0.89
Model 1-pinned connections	1.00	2.00	0.29	0.43	0.4	4E-04	6.8E-04	3.36
Model 2-rigid connections	1.00	2.10	0.30	0.43	0.8	1E-04	1.8E-04	0.91
Model 2-pinned connections	1.00	2.39	0.34	0.43	0.46	3E-04	9.4E-04	4.59
Model 3-rigid connections	1.00	2.04	0.30	0.43	0.46	3E-04	5.3E-04	2.61
Model 3-pinned connections	1.00	1.96	0.30	0.43	0.25	2E-03	3.1E-03	15.68

Table 16 shows that for the case study structures, the probability of exceedance in 50 years is small under severe earthquakes. For stiff systems due to the existence of curves with high spectral acceleration and the minimum relative displacement, and for relative displacement capacity, there are large corresponding spectral accelerations, which result in a small annual exceedance probability according to the area hazard curve

CONCLUSION

The Platforms IDA curves show that, in general, in these structures even at high intensity levels, no global dynamic instability is observed. Statistical analysis of the results from seismic reliability analysis shows that all platforms with rigid connections can provide the desired performance level of FEMA for the collapse prevention. The results of reliability analysis indicate that amongst the pinned platforms, only one provides the desired confidence level of FEMA due to its special geometry. Structures with pinned connections show softer behavior compared with structures with rigid connections, and reach the performance level of collapse prevention at lower spectral accelerations. These structures also have a lower confidence level. Considering the median demand for these platforms at the time of applying the corresponding spectral acceleration with the risk level of 2% in 50 years and considering the area risk curve, the levels of annual exceedance probability of the performance

level of collapse prevention are very small.

REFERENCES

- Abdollahzadeh, G. and Malekzadeh, H. (2013). "Response modification factor of coupled steel shear walls", *Civil Engineering Infrastructures Journal*, 46(1), 15-26.
- Abdollahzadeh, G., Sazjini, M. and Asghari, A. (2015). "Seismic fragility assessment of special truss moment frames (STMF) using the capacity spectrum method", *Civil Engineering Infrastructures Journal*, 48(1), 1-8.
- Ajamy, A., Zolfaghari, M.R., Asgarian, B. and Ventura, C.E. (2014). "Probabilistic seismic analysis of offshore platforms incorporating uncertainty in soil-pile-structure interactions", *Constructional Steel Research journal*, 101, 265-279.
- American Petroleum Institute. (2000). "Recommended practice for planning, designing and constructing fixed offshore platforms-working stress design", API Recommended Practice 2A-WSD (RP 2A-SD), 21th Edition, December 2000, Washington D.C., USA.
- Asgarian, B., Aghakouchak A.A., Alanjari, P. and Assareh, M.A. (2008). "Incremental dynamic analysis of jacket type offshore platforms considering soil-pile interaction", *The 14th World Conference on Earthquake Engineering*, October 12-17, Beijing, China.
- Asgarian, B., Sadrinezhad, A. and Alanjari, P. (2010). "Seismic performance evaluation of steel moment resisting frames through incremental dynamic analysis", *Constructional Steel Research journal*, 66, 178-190.
- Asgarian, B., Salehi Golsefid, E. and Shokrgozar, H.R. (2016). "Probabilistic seismic evaluation of buckling restrained braced frames using DCFD and PSDA methods", *Earthquakes Structures*, 10(1), 105-123.
- Asgarian, B., and Ajamy, A. (2010). "Seismic performance of jacket type offshore platforms through incremental dynamic analysis", *Offshore Mechanics and Arctic Engineering Journal*,

- 132(3), 31-47.
- Bertero, V.V. (1977). "Strength and deformation capacities of buildings under extreme environments", *Structural Engineering and Mechanics*, Pister K.S. (ed.), Prentice-Hall: Englewood Cliffs, NJ, 211-215.
- Bertero, R.D. and Bertero, V.V. (2002). "Performance-based seismic engineering: The need for a reliable conceptual comprehensive approach", *Earthquake Engineering and Structural Dynamic*, 31(3), 627-652.
- Bayat, M., Daneshjoo, F. and Nisticò, N. (2015). "A novel proficient and sufficient intensity measure for probabilistic analysis of skewed highway bridges", *Structural Engineering and Mechanics*, 55(6), 1177-1202.
- Bayat, M., Daneshjoo, F., Nisticò, N. and Pejovic, J. (2017). "Seismic evaluation of isolated skewed bridges using fragility function methodology", *Computers and Concrete*, 20(4), 419-427.
- Dastan Diznab, M.A., Mohajernassab, S., Seif, M.S., Tabeshpour, M.R. and Mehdigholi, H. (2014). "Assessment of offshore structures under extreme wave conditions by modified endurance wave analysis", *Marine Structures*, 39, 50-69.
- Davani, M.R., Hatami, S. and Zare, A. (2016). "Performance-based evaluation of strap-braced cold-formed steel frames using incremental dynamic analysis", *Steel and Composite Structures*, 21(6), 1369-1388.
- Federal Emergency Management Agency. (2000). "FEMA-355F, state of the art report on performance prediction and evaluation of steel moment-frame buildings", Washington D.C., USA.
- Golafshani, A.A., Tabeshpour, M.R. and Komachi, Y. (2009). "FEMA approaches in seismic assessment of jacket platforms, Case study: Ressalat jacket of Persian Gulf", *Journal of Constructional Steel Research*, 65(10), 1979-1986.
- Golafshani, A., Ebrahimian, H., Bagheri, V. and Holmas, T. (2011). "Assessment of offshore platforms under extreme waves by probabilistic incremental wave analysis", *Journal of Constructional Steel Research*, 67(10), 759-769.
- Hamburger, R.O. and Moehle, J.P. (2002). "State of performance-based engineering in the United States", Technical Report, University of California, Berkeley, USA.
- Hezarjaribi, M., Bahaari, M.R., Bagheri, V. and Ebrahimian, H. (2013). "Sensitivity analysis of jacket-type offshore platforms under extreme waves", *Journal of Constructional Steel Research*, 83, 147-155.
- Ibarra, L.F. and Krawinkler, H. (2005). "Global collapse of frame structures under seismic excitations", PEER Report 2005/06, Pacific Earthquake Engineering Research Center, University of California, Berkeley, USA.
- Jalayer, F. and Cornell, C.A. (2000). "A technical framework for probability-based demand and capacity factor (DCFD) seismic formats", Report No. RMS-43, RMS Program, Stanford University, Stanford, USA.
- Kim, T.W., Foutch, D., LaFave, J. and Wilcoski, J. (2004). "Performance assessment of reinforced concrete structural walls for seismic load", Structural Research Series No. 634, Department of Civil and Environmental Engineering, University of Illinois at Urbana-Champaign Urbana, Illinois.
- Komachi, Y., Tabeshpour, M.R. and Golafshani, A.A. (2009). "Assessment of seismic vulnerability of jacket platforms based on the performance", *11th International Conference of Ocean Industries*, Kish, Iran (in Persian).
- Khorami, M., Khorami, M., Motahar, H., Alvansazyazdi, M., Shariati, M., Jalali, A. and Tahir, M.M. (2017). "Evaluation of the seismic performance of special moment frames using incremental nonlinear dynamic analysis", *Structural Engineering and Mechanics*, 63(2), 259-268.
- Lee, Y.J. and Moon, D.S. (2014). "A new methodology of the development of seismic fragility curves", *Smart Structures and Systems*, 14(5), 847-867.
- Mahmoudi, M., Vatani Oskouie, A. and Havaran, A. (2013). "The effect of easy-going steel on KBF's seismic behavior", *Civil Engineering Infrastructures Journal*, 46(1), 81-94.
- Management and Planning Organization of Iran. (2006). "Ports and marine structures design manual (Marine Jackets)", No: 300-9, Tehran, Iran (in Persian).
- Maniyar, M.M., Khare, R.K. and Dhakal, R.P. (2009). "Probabilistic seismic performance evaluation of non-seismic RC frame buildings", *Structural Engineering and Mechanics*, 33(6), 725-745.
- Mirtaheri, M., Amini, M. and Khorshidi, H. (2017). "Incremental dynamic analyses of concrete buildings reinforced with shape memory alloy", *Steel and Composite Structures*, 23(1), 95-105.
- Pourgharibshahi, A. and Hadavand Khani, A. (2011). "Seismic reliability assessment of jacket offshore platforms", *The 13th Marine Industries Conference (MIC2011)*, 8-11 November, Kish Island, Iran.
- Qiao, S., Han, X., Zhou, K. and Li, W. (2017). "Conceptual configuration and seismic performance of high-rise steel braced frame", *Steel and Composite Structures*, 23(2), 173-186.
- Seismosoft. (2013). "SeismoStruct v6.5: A computer program for static and dynamic nonlinear analysis of framed structures", available from <http://www.seismosoft.com>.

- Sistani, A., Asgarian, B. and Jalaeefar, A. (2013). "Reliability analysis of braced frames subjected to near field ground motions", *Earthquake Structures*, 5(6), 733-751.
- Soleimani, M. and Nurzad, A. (2012). "Seismic hazard dissection and estimation of probable earthquake scenarios in Pars specified economic region", *9th International Civil Engineering Congress*, Isfahan University of Technology, Iran (in Persian).
- Taucer, F.F., Spacone, E. and Filippou, F.C. (1991). "A Fiber beam-column element for seismic response analysis of reinforced concrete structures", Earthquake Engineering Research Center, Report No. UCB/EERC-91/17, December 1991. University of California, Berkeley, USA.
- Terzic, V. (2011). "Force-based element vs. displacement-based element", University of California, Berkeley, USA, December.
- Vamvatsikos, D. and Cornell, C.A. (2002). "The incremental dynamic analysis and its application to performance-based earthquake engineering", *12th European Conference on Earthquake Engineering*, London, Paper No. 479.
- Waseem, M. and Spacone, E. (2017). "Fragility curves for the typical multi-span simply supported bridges in northern Pakistan", *Structural Engineering and Mechanics*, 64(2), 213-223.
- Yön, B. (2016). "An evaluation of the seismic response of symmetric steel space buildings", *Steel and Composite Structures*, 20(2), 399-412.